Available online at www.sciencedirect.com
ScienceDirect
ELSEVIER
Nuclear Instruments and Methods in Physics Research A 579 (2007) 951–960
NUCLEAR INSTRUMENTS & METHODS IN PHYSICS RESEARCH Section A
www.elsevier.com/locate/nima

Results of the first integration test of the CMS drift tubes muon trigger

M. Aldaya[a], N. Amapane[b], S. Argirò[b], C. Battilana[c], R. Bellan[b], M. Bellato[d], A. Benvenuti[c], M. Boldini[c], S. Bolognesi[b], M. Bontenackels[e], E. Borsato[d], S. Braibant[c], V. Cafaro[c], P. Capiluppi[c], L. Castellani[d], F.R. Cavallo[c], G. Cerminara[b], M. Cerrada[a], P. Checchia[d], E. Conti[d], B. de la Cruz[a], F. Dal Corso[d], G.M. Dallavalle[c], C. Deldicque[g], G. Dellacasa[b], J. Erö[g], A. Fanfani[c], C. Fernández[a], J. Fernández de Trocóniz[f], M.C. Fouz[a], F. Gasparini[d], U. Gasparini[d], P. Giacomelli[c], V. Giordano[c], M. Giunta[c], F. Gonella[d], L. Guiducci[c], T. Hebbeker[e], K. Hoepfner[e], I. Jiménez[f], I. Josa[a], S. Lacaprara[h], I. Lippi[d], S. Marcellini[c,*], C. Mariotti[b], G. Maron[h], S. Maselli[b], G. Masetti[c], A.T. Meneguzzo[d], G. Mila[b], V. Monaco[b], A. Montanari[c], F. Navarria[c], M. Nervo[b], F. Odorici[c], A. Parenti[d], M. Passaseo[d], M. Pegoraro[d], G. Pellegrini[c], A. Perrotta[c], J. Puerta[g], H. Reithler[e], A. Romero[b], L. Romero[a], P. Ronchese[d], A. Rossi[c], T. Rovelli[c], P. Ruetten[e], R. Sacchi[b], G.P. Siroli[c], M. Sowa[e], A. Staiano[b], N. Toniolo[h], E. Torassa[d], G. Torromeo[c], R. Travaglini[c], V. Vaniev[b], S. Vanini[d], S. Ventura[d], C. Villanueva[a], C. Willmott[a], M. Zanetti[d], P. Zotto[d], G. Zumerle[d]

[a]*CIEMAT - División de Física Experimental de Altas Energías, Avenida Complutense 22, E 28040 Madrid, Spain*
[b]*Dipartimento di Fisica dell'Università e Sezione INFN di Torino, Via Giuria 1, I 10125 Torino, Italy*
[c]*Dipartimento di Fisica dell'Università e Sezione INFN di Bologna, Viale Berti Pichat 6/2, I 40127 Bologna, Italy*
[d]*Dipartimento di Fisica dell'Università e Sezione INFN di Padova, Via Marzolo 8, I 35131 Padova, Italy*
[e]*III. Physikalisches Institut der RWTH Aachen, D 52056 Aachen, Germany*
[f]*Universidad Autónoma de Madrid, Ctra. de Colmenar km 15, E 28049 Madrid, Spain*
[g]*Institute for High Energy Physics of the Austrian Academy of Sciences, Nikolsdorfergasse 18, A 1050 Wien, Austria*
[h]*INFN, Laboratori Nazionali di Legnaro, Viale dell'Università 2, I 35020 Legnaro (PD), Italy*

Received 16 May 2007; accepted 6 June 2007
Available online 13 June 2007

Abstract

Two drift tubes (DTs) chambers of the CMS muon barrel system were exposed to a 40 MHz bunched muon beam at the CERN SPS, and for the first time the whole CMS Level-1 DTs-based trigger system chain was tested. Data at different energies and inclination angles of the incident muon beam were collected, as well as data with and without an iron absorber placed between the two chambers, to simulate the electromagnetic shower development in CMS. Special data-taking runs were dedicated to test for the first time the Track Finder system, which reconstructs track trigger candidates by performing a proper matching of the muon segments delivered by the two chambers. The present paper describes the results of these measurements.

PACS: 29.40.Gx; 07.05.Hd

Keywords: LHC; CMS; Drift-tubes; Trigger; Muon detector

*Corresponding author. Tel.: +39 0512095238; fax: +39 0512095269.
E-mail address: Stefano.Marcellini@bo.infn.it (S. Marcellini).

0168-9002/$ - see front matter © 2007 Elsevier B.V. All rights reserved.
doi:10.1016/j.nima.2007.06.007

1. Introduction

The task of the muon trigger of the CMS experiment at LHC [1–3] is to provide muon identification and to measure the particle transverse momentum, in order to allow online rate reduction. In addition the system has to assign to each muon candidate the corresponding pp collision bunch crossing (BX) already at the hardware level, called Level-1 trigger. In the barrel region of the CMS detector, the muon trigger is delivered independently by two subsystems: the resistive plate chambers (RPC) and the drift-tubes (DTs) chambers. Whereas the RPC detector has an excellent time resolution from single hits, which corresponds to a very precise and unambiguous BX determination, accompanied by less precise momentum and position resolution, the DT system can perform a precise momentum measurement associated with good BX determination based on a fast track reconstruction.

In each muon station the DT local trigger in the r–ϕ view, which is the bending plane, provides up to two track segments (trigger primitives) for each BX. Then the DT Track-Finder (DTTF) system constructs a muon track candidate by performing a proper matching between the segments delivered by the local trigger in the DT muon stations crossed by the particle. A BX is assigned to the muon trigger candidate, as well as a transverse momentum value p_t.

In order to test and validate the performance of the barrel muon chamber readout and trigger electronics, a bunched beam is needed, with a time structure similar to the one at the LHC, where proton collisions occur every 25 ns, corresponding to a frequency of 40 MHz. A complete test of the DT local trigger electronics and of the performance of the corresponding local trigger was made in May 2003 at the CERN SPS using an LHC-like muon beam to which a single muon station was exposed. The results of the measurements performed in this test are described in Ref. [4].

An experimental set-up consisting of two muon stations, both equipped with the DT trigger and read-out electronics, was exposed to a muon beam synchronized with a clock of 40 MHz frequency, and having the same characteristics of the previous test. This allowed to have muons crossing the experimental apparatus at time intervals which were multiples of 25 ns, and synchronized with the BX frequency expected at LHC. The main difference from previous test-beams was that the output of the local trigger of the two muon stations was sent as input to the DTTF, and the whole DT Level-1 trigger chain was then tested for the first time. No magnetic field was available for the measurements. In order to simulate the bending of the muon tracks in the CMS magnetic field, one station was shifted and tilted with respect to the other. Data were taken at several incident track inclination angles and momenta, with and without an iron absorber placed between the two muon stations, to reproduce the effect of the material in CMS. This allowed to study the impact of the electromagnetic showers on the trigger performance. This paper reports the results of these measurements.

2. The DTs local trigger

The CMS muon barrel drift chambers are described extensively elsewhere [5]. They are composed of three groups of DTs called superlayers (SLs). Each SL is built of four layers of DTs, staggered by half a tube width. Two SLs measure muons in the transverse bending plane (r–ϕ) of CMS (hereafter ϕ view) and one SL detects them in the longitudinal non-bending (r–θ) plane (hereafter θ view). The two ϕ SLs are called "inner" or "outer" to identify their position with respect to the center of CMS in the muon station where they are located. A honeycomb panel to give stiffness to the chamber, and a θ SL, separate the two ϕ SLs and provide a lever arm for a better track angular resolution. The CMS muon barrel is assembled in such a way that muon tracks produced in LHC interactions can cross up to four muon stations, placed at different distances from the interaction point. The stations are labeled MB1, MB2, MB3 and MB4, starting from the center of CMS. Each chamber is instrumented with read-out electronics, as well as with bunch and track identifiers (BTIs), track correlators (TRACOs) and trigger server (TS), which are the basic elements of the DT local trigger chain. The block scheme of the DT electronics mounted on each muon station is shown in Fig. 1. Details can be found in Ref. [4] and references therein.

The DT local trigger provides the DT trigger primitives for the muon trigger, and its logical steps are now summarised. The basic elements to form the trigger primitives are the segments provided by the BTIs in the three SLs separately. Each BTI unit reads nine DT cells, and the BTIs are arranged one next to the other in such a way that there is always an overlap of five cells between two adjacent units. The BTI searches for a spatial alignment of at least three hits in the DTs within a SL. If the alignment is detected, a BTI segment is found. As the BTI system has a well defined latency time, the time when the alignment occurs in the electronics also defines the BX at which the event has occurred, which is then assigned to the segment itself. The BTI assigns a quality tag to the segment, which is High (H) or Low (L) if an alignment of hits in all the four layers of the SL is found, or in only three out of four layers, respectively. The inner and outer segments in the ϕ view of a muon station can be found correlated by the TRACOs if a spatial matching between BTIs segments of the inner and outer SLs is found at the same BX. The TRACO also assigns a quality to the segment, which can be HH, HL, or LL, where H and L is the quality of the matched segments. If the correlation fails, or if one of the two BTIs segments is simply missing, the trigger candidate found by the TRACO will be from one SL only, with quality Ho, Hi, Lo or Li, where "o" and "i" stand for "outer" and "inner", respectively. A local trigger segment is also characterized by the "radial angle" ϕ, and

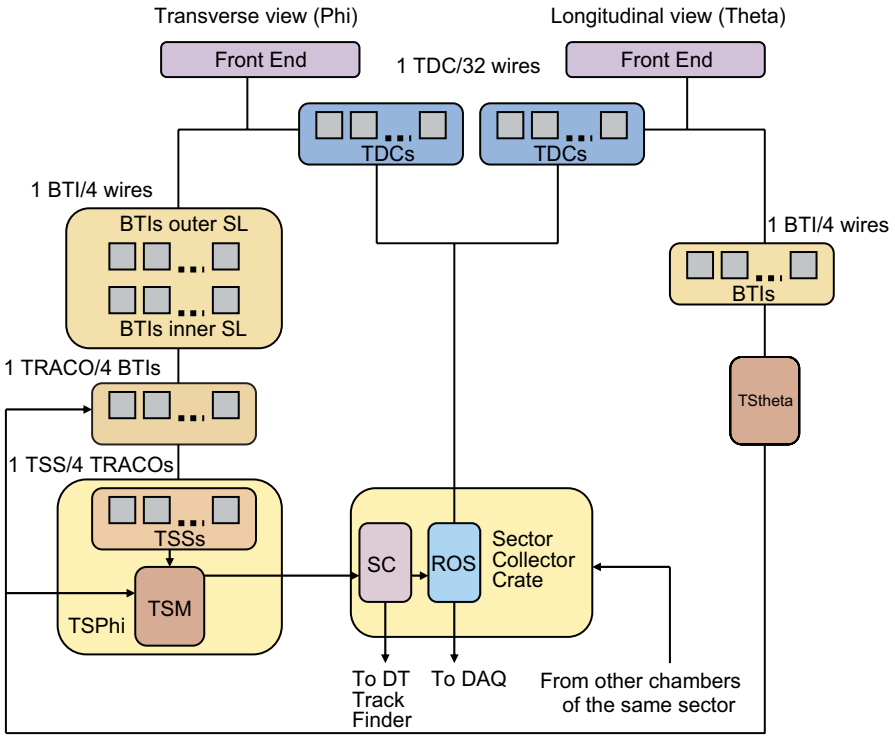

Fig. 1. Overview of the main building blocks of a barrel muon station electronics. Transverse and longitudinal view labels correspond to ϕ and θ view, respectively.

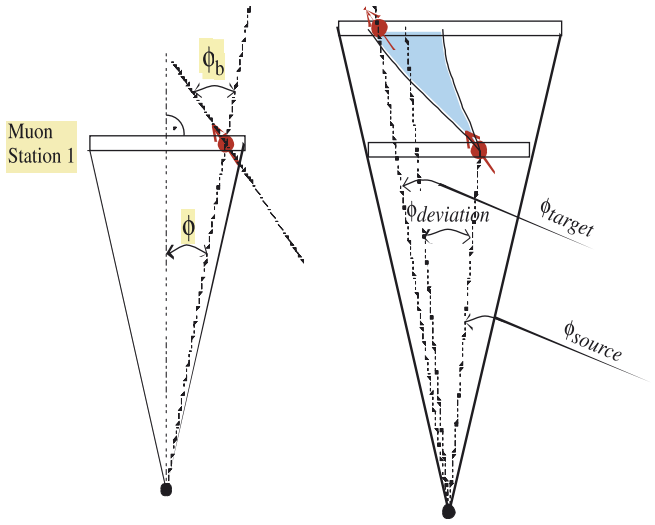

Fig. 2. A sketch of the quantities ϕ and ϕ_b which are delivered by the DT local trigger to the DTTF in each muon station, to construct a track candidate, are shown in the leftmost figure. The angle ϕ, also called "radial angle", defines the displacement of the trigger segment with respect to the center of the muon station. The angle ϕ_b, also called "bending angle", is the angle of the trigger segment with respect to the direction of a track with infinite transverse momentum, crossing the muon station in that position. The rightmost figure shows in a schematic way how DT local trigger segments from a station are extrapolated to another station by the DTTF in the ϕ view.

the "bending angle" ϕ_b, which are sketched in Fig. 2. Due to the size of the muon chambers, on average there are about 20 TRACOs per chamber, being 24 for in largest station. Each TRACO can deliver up to two track candidates to the TS, related to the same physical BX and this is done for any BX. In the case of the test-beam, a physical BX is a single beam shot. Each TRACO labels its two candidates as "first" and "second" track, using a programmable priority encoding. The two tracks are multiplexed on the same bus, and therefore the second track will be transferred one BX later if there is no new trigger in this next BX.

The TS has to select up to two track segments for each BX, out of the average number of 40 segments delivered by all the TRACOs in each station.[1] The two segments selected by the TS should correspond, from the physics point of view, to the two tracks with highest transverse momentum. In practice the sorting algorithm is based on both the quality of the track segments and their bending angle. Due to functional redundancy introduced in BTIs and TRACOs for system robustness, segment copies can be generated by the device when a single track traverses a muon chamber. Therefore, several ghost suppression mechanisms are applied by the local trigger, to get rid of such segment copies. Since the chamber trigger electronics delivers as output at most two muon candidates, ghost track rejection will be very important for reliably selecting di-muon events in LHC pp collisions, in the case the two muons are very close in space.

A relevant feature of the θ trigger is to validate uncorrelated low quality segments delivered by the ϕ

[1] In normal cases most of such segments will be null tracks.

trigger. Such type of segments are in fact delivered by the local trigger to the regional trigger only if a θ trigger segment is also found in the same station at the same BX.

3. The DTTF trigger

A detailed description of the DTTF trigger system can be found in Ref. [3]. The task of the DTTF is to find muon tracks in the barrel region originating from the interaction point, and to measure their transverse momentum and their location in pseudorapidity θ and azimuthal angle ϕ at the hardware level. The DTTF reconstructs muon candidates by matching track segments from different stations. After the track-finding process, the DTTF system assigns to the muon track candidate a transverse momentum measurement, a ϕ and θ coordinate measurement, and a quality word.

The Sector Collector (SC) is the device which collects the DT trigger segments from the chambers of a muon sector, and delivers them to the DTTF. For each BX, in the ϕ view, a maximum of two trigger segments per station can be delivered by the SC to the DTTF, whereas only one track segment per BX is delivered in the θ view. The DTTF then attempts to construct track candidates by matching the segments from each muon station as sketched in Figs. 2 and 3.

The DTTF track-finding algorithm is performed by the Phi Track-Finder (PHTF) processors, which find tracks in the transverse plane (ϕ view), and the Eta Track-Finder (ETTF) processors, which find tracks in the longitudinal plane (θ view). The PHTF algorithm can be described as a three-step process. First the extrapolation unit tries to match track segment pairs of distinct muon stations within the same sector, or within neighboring sectors, using a pairwise matching method. This is performed by extrapolating a track segment to the next station, using the spatial and angular measurement ϕ and ϕ_b of the track segment itself previously defined. The matched pairs are then forwarded to the track assembler unit, which links the segment pairs to full tracks. The assignment unit performs the last step, determining the track parameters for each trigger candidate. The ETTF then promotes the PHTF tracks, measured only in the transverse plane, to full 3D muon candidates.

Finally, the wedge sorter and the barrel sorter select the four highest transverse momentum tracks in the barrel detector and forward them to the global muon trigger.

4. Experimental set-up and collected data

The experimental set-up consisted of two DT barrel muon chambers arranged as in Fig. 4, where the top view is shown. The whole system was installed in the H2 zone of the CERN SPS North Area and exposed to a secondary muon beam with momentum varying from 30 to 300 GeV/c. The test was carried out using the SPS radio frequency structure similar to the one foreseen at the LHC. The proton beam delivered by the SPS hit a primary target in narrow bunches (about 2 ns long, separated by 25 ns) generating muons. From these muons a secondary beam with the same time structure of the proton primary beam was formed, by selecting the proper particle momentum. Trains of 48 bunches occurred every 25 μs during a spill of 2.2 s length (a so called slow-extraction cycle of the SPS). Since a secondary beam was used, the mean muon occupancy in a bunch was rather low, of the order of

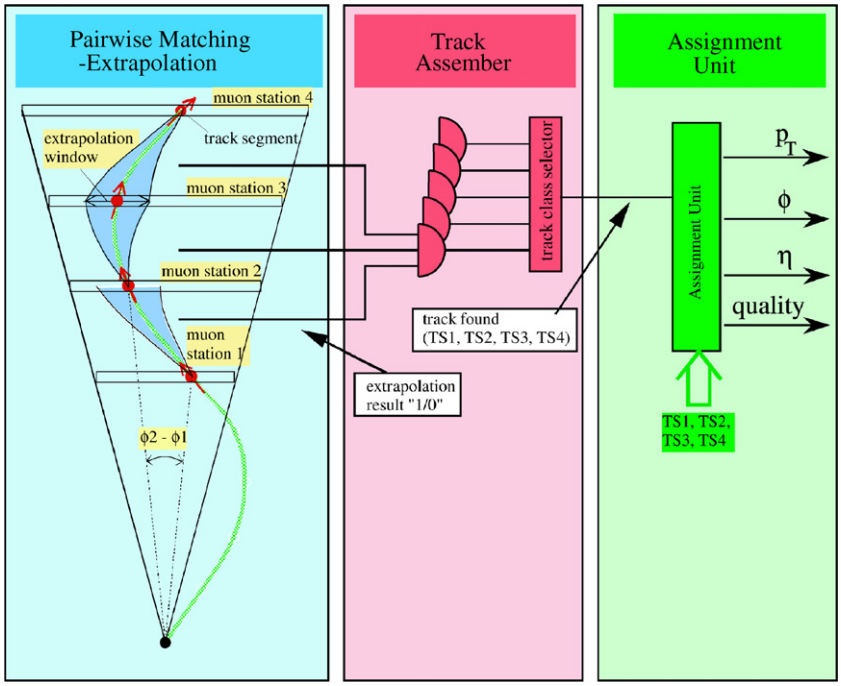

Fig. 3. A scheme of the logical processes of the DT Track-Finder algorithm.

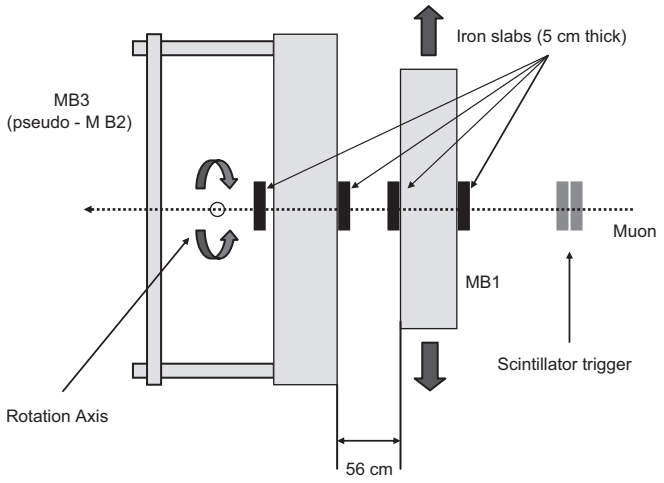

Fig. 4. A top-view sketch of the experimental set-up. The muon beam direction is shown by the arrow. The bending of the muon track in the CMS magnetic field was simulated by rotating MB3, whose rotation axis of MB3 is orthogonal to the plane of the figure. MB1 could be shifted orthogonally to the beam direction, as shown by the arrows.

10^{-2}–10^{-3}, and therefore muons were separated in time by several microseconds on average. The 40 MHz signal, synchronous with the accelerator RF signal, was distributed in the experimental area via a TTC system [6] through optical links, and it was used as clock signal for the trigger electronics. Both chambers had the ϕ view wires in the vertical direction. The up-stream chamber with respect to the muon beam was an MB1 type chamber. It was placed on a support which allowed lateral displacement in the direction perpendicular to the beam direction. The down-stream chamber was an MB3 type chamber, placed on a mechanical support which allowed rotation around its central vertical axis, as well as any horizontal displacement. A proper rotation and displacement of the MB3 chamber with respect to MB1 allowed to simulate the bending of the muon tracks in the CMS magnetic field. Both chambers were equipped with minicrates with the related read-out and trigger electronics. The trigger electronics was configured mocking an MB2 type station for MB3. Therefore, from the point of view of the trigger, an MB1 and an MB2 muon stations of the central wheel of the CMS detector were tested. The chambers were flushed with an Ar/CO_2 (85%/15%) gas mixture with a gas flow of 2 l/min. The oxygen concentration was measured by an oxygen monitor placed downstream before the gas exhaust and was always below 100 ppm during data taking. The high voltage values of the electrodes were: $V_{wire} = 3600\,V$, $V_{strip} = 1800\,V$, $V_{cathode} = -1200\,V$. The discrimination threshold of the front-end readout electronics was set to 15 mV, corresponding to about 4.5 fC. The setup discrimination threshold and HV values were those foreseen for operation at the LHC.

In order to simulate the effect of the material in the CMS muon detector, two iron slabs, 5 cm thick each, were placed between the two stations. Two additional iron slabs, each 5 cm thick, were placed one in front of MB1, and one behind MB3, the latter to simulate back-scattering. Concrete blocks were located about 40 cm up-stream the two trigger scintillators during the whole data-taking.

Each of the two DT chambers delivered its local trigger data to a prototype of the trigger DT sector collector VME board. At the sector collector level the trigger data were reduced (i.e. null tracks were rejected), synchronized and fanned out to both a pattern unit [7] and to a prototype of the PHTF processor. The local DAQ acquired trigger data from the pattern unit. The DTTF delivered its trigger track candidates to a prototype of the DT wedge sorter board, whose data output was recorded in a second pattern unit and read out via the DAQ. Two track candidates for each BX were delivered as output by the whole system. Full information about all steps of the DTTF track-finding process in 10 BXs around the trigger was accessed using a special VME-JTAG local readout system called Spy-DAQ. The trigger electronics system used in the test beam had prototypes of all the constituents of the CMS DT trigger system, with the exception of optical links from the sector collector to the DTTF: however those links do not perform any processing, and optical transmission was thoroughly tested independently.

An external beam trigger was given by the coincidence of two plastic scintillators defining a $10 \times 10\,cm^2$ area and almost fully covering the muon beam. Details of the electronics and data read-out system of the experimental set-up can be found in Ref. [4]. During the data taking, the hardware of the local trigger was set-up with the default configuration expected at LHC. Data were collected scanning different inclination angles of the MB3 type chamber, from -30° to $+30^\circ$, in steps of 10°. The effect of the material placed between the two stations was studied using data collected with and without the iron absorbers, and at different muon beam energies, in the range from 50 to 300 GeV/c. This subset of data were collected with beam at normal incidence.

5. Experimental results

In this section the experimental results on the performance of the trigger system obtained in the test will be described. In addition to further measurements related to the local trigger (which was already tested several times in the past, as described in Ref. [4] and references therein) this paper also reports the results of the DTTF system, whose hardware was tested for the first time with a bunched beam.

The muon local trigger system was designed to provide a high trigger efficiency, a correct identification of the BX, and a very low ghost rate. The system must also deliver the reconstructed trigger segments with the position and bending angle of the crossing particle. Ghosts are copies of the trigger segment at the correct BX, as well as fake triggers at the wrong BX. They may originate from wrong alignment of hits in a DT muon station, due to the presence

of extra hits produced by electromagnetic cascades and δ-rays, or from redundancies in the trigger electronics. Such features can be accurately tested by selecting events with single muons crossing the experimental apparatus at different incident angles. Results with and without the iron absorber placed between the two chambers, and as a function of the beam energy will be shown.

The DTTF system has to match in the proper way the trigger segments delivered by the two muon stations, and produce a track. It also has the task to suppress, at its output, the ghost rate produced by the single muon stations at wrong BX, still keeping high efficiency for segment matching at the correct BX. The performance of the DTTF was tested using single muon events. As the trigger to the DAQ was given by the coincidence of two plastic scintillators, any selected event was required to have a signal in this device within a time window of ±2 ns from the expected peak position.

5.1. DTs local trigger results

Single muon events were selected by applying the selection cuts in the MB1 station, which was up-stream with respect to the beam, allowing to use the MB3 station to study the trigger performance in an unbiased manner.

The quantity t_0 is defined as the TDC time corresponding to hits issued by tracks crossing the DT at the wire position. The presence in the events of recorded TDC hits within a 500 ns time window after t_0 on at least three cells, in the region of the ϕ view of MB1 illuminated by the beam, was required in order to reject events with fake scintillator coincidence.

The BTI has a programmable dead time that protects the computations in case of multiple hits on the same cell (due to afterpulses, electromagnetic background or multiple beam tracks). The first detected hit on each BTI raises a flag that rejects signals from late hits within a programmable time window (by default set equal to the maximum drift time $T_{\max}$). Only hits detected in the range $-T_{\max} < t_0 < 2T_{\max}$ can affect the BTI calculations and are actually relevant for trigger: hits arriving in this time range earlier than the one corresponding to the muon will mask it, modifying the trigger decision, while hits coming afterward will restart the BTI calculations adding noisy triggers. Therefore, the sample can be cleaned from events with out-of-time muons by asking for less than three hits outside this time window in the ϕ view of the MB1 chamber, without introducing any bias in the trigger decision. For this purpose, $T_{\max}$ was approximated to 400 ns. Nevertheless, a relevant number of events with two muons are still left in this selection, mainly due to the large time window allowed. To improve the single muon selection, and reject events with two muons crossing the same DT cell, events were discarded if more than six cells with hits (within the selection time window) were found in any of the three SLs. In summary, the single muon event selection cuts were the following:

- scintillator trigger time with ±2 ns tolerance around the average time;
- at least three cells with recorded hits in the beam region, in the ϕ view of MB1, with recorded TDC time within 500 ns from the t_0 of the event;
- less than three hits recorded outside the time interval range $-400 < t_0 < 800$ ns in the ϕ view of MB1; and
- a maximum of six cells with hits in every SL of MB1.

Typically about 65% of the triggered events pass the single muon selection cuts. A different single muon event selection was also tested, to check the presence of bias in the event selection. Events were required to have a HH trigger segment in MB1 at the correct BX, and exactly eight cells with hits in the ϕ view of the same station. Such requirements are more stringent than the ones listed above, and in principle should allow to select a cleaner sample of isolated muons crossing the experimental set-up at the correct time. Nevertheless, no relevant systematic differences are observed in the experimental results when the two selections are compared.

TDC hits were fitted by the CMS reconstruction program, especially adapted for the test beam data. Fitted track segments resulting from aligned TDC hits were found in each muon chamber separately, and independently from the local trigger results.

Statistical errors were computed for every measurement and included in the plots throughout the paper, although their size are smaller than the points themselves and are not visible.

The BX identification efficiency is defined as the fraction of selected single muon events for which the local trigger delivered at least one trigger segment at the correct BX and it is shown in Fig. 5 as a function of the beam incident angle. Data used to obtain this plot were collected with no iron absorber between the two muon stations. The lower

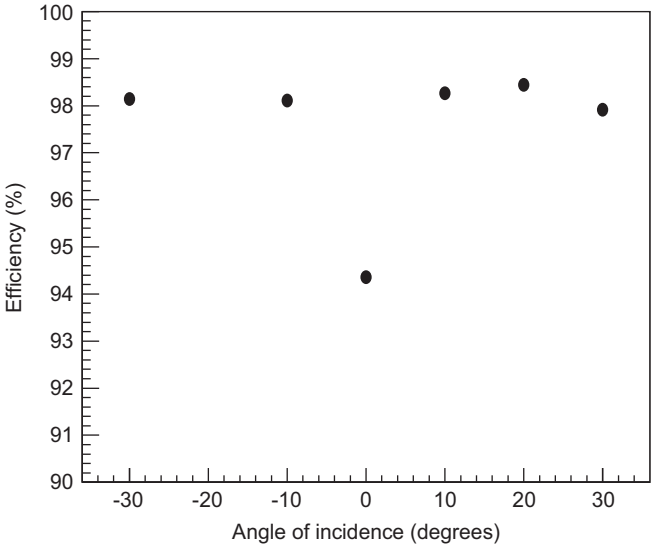

Fig. 5. BX identification efficiency in MB3 for single muon events, as a function of the particle incident angle.

efficiency at 0° is a pure geometrical effect due to the staggering of the drift cells: as at least three hits in a SL are required to provide a trigger, at normal incidence it is higher the probability for a track to cross the detector in the dead area between the cells, in at least two layers.

In the case of single muon events, if two trigger segments are delivered at the same BX by the local trigger system in a muon station, the second trigger is considered a ghost copy of the first one. Although generally with a poorer quality, ghosts at the correct BX reproduce the characteristics of the main trigger segment in terms of position and angle. Fig. 6 shows the fraction of ghost triggers per event, defined as the fraction of single muon events with two triggers at the correct BX in MB3, as a function of the beam incident angle. The data taking conditions were the same as for Fig. 5. The ghost rate in the trigger data is symmetric, for positive and negative incident angles, within about 15%. At this stage it should be mentioned that the ghost rate measurements are sensitive to systematic effects related to the position crossed by the particle within the BTI or the TRACO, combined to its inclination. This is because the geometrical position of the drift-cells in the BTI is not symmetric with angle. This effect is very small on average, if the chamber is uniformly illuminated, but it can become visible if, as in this case, the beam spot is only few centimeters wide, and it can be enhanced by the inclination of the track.

The production of segments associated to a wrong BX, arising from wrong hit alignment, is intrinsic of the BTI algorithm. In addition there are also cases in which the hit alignment is spoiled by δ-ray production or electromagnetic shower. Such fake triggers, which are called "out-of-time" ghosts, are almost entirely uncorrelated low quality segments, and are distributed over a wide range of BXs. In Fig. 7 the measured fraction of out-of-time triggers per event is shown as a function of the beam incident angle. The asymmetry between positive and negative angles are explained by the BTI geometry explained above.

The effect of the iron absorber placed between the two muon stations is the enhancement of the probability for a high momentum muon to produce electromagnetic showers. Such probability also increases as a function of the muon momentum. This has the effect to decrease the BX identification efficiency, and to increase the noise rate, and therefore to partially reduce the trigger capability of the system. The BX identification efficiency for the MB3-type station is shown in Fig. 8 as a function of the muon momentum, for events with and without the iron absorber. Data used for this plot were collected at normal beam incidence. The expected efficiency drop is observed when the iron slabs are inserted between the two chambers, and it amounts to about 1% at 50 GeV muon momentum, increasing up to about 1.6% at 300 GeV, which still guarantees the expected DT trigger performance.

An efficiency loss as a function of the increasing momentum, in the case of no absorber in front of MB3, is also observed. Several effects may account for it, although it is difficult to quantify their relative contribution. It was observed that the characteristics of the beam were different for different beam energies: in particular the angular dispersion of the beam was larger for low energy. In the case of normal incidence, a larger angular dispersion reduces the geometrical effects due to the staggering of the drift cells (as shown in Fig. 5) thus increasing the trigger efficiency. In addition the electromagnetic showers induced by the presence of the material in MB3 itself may also play

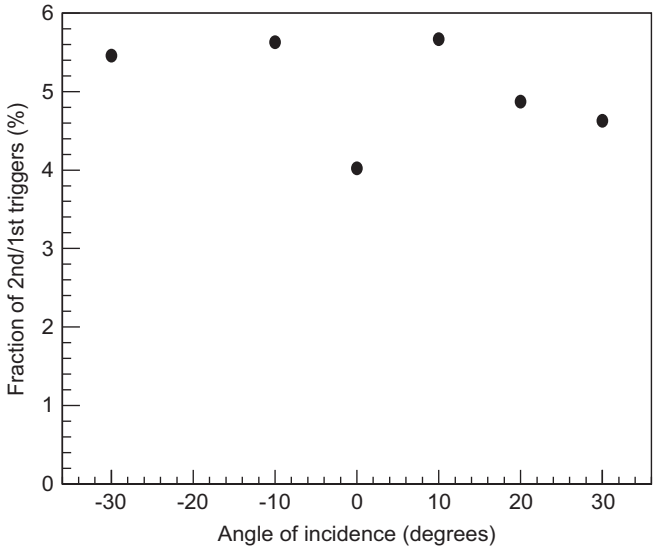

Fig. 6. Fraction of ghost triggers observed in MB3, defined as the ratio of the number of second tracks over the number of first tracks, delivered by the local trigger at the correct BX, as a function of the beam incident angle, for single muon events.

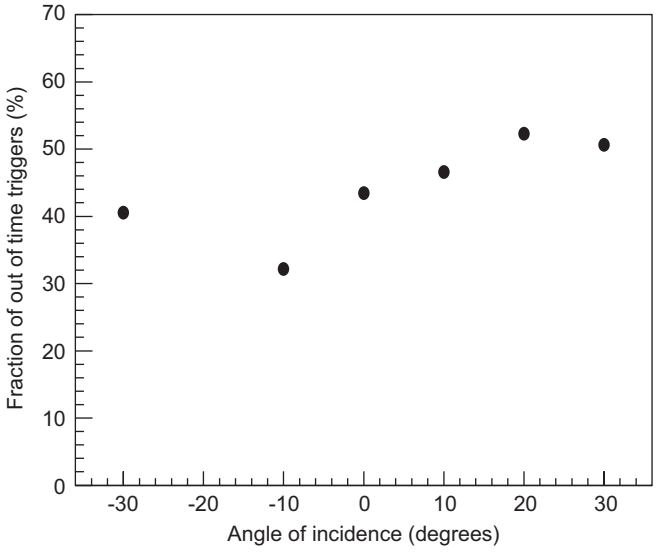

Fig. 7. The fraction of out-of-time triggers per event observed in MB3, defined as the total number of such triggers divided by the number of in-time triggers, as a function of the beam incident angle. Measurements discussed in Section 5.2 show that the ghosts at the output of the local trigger are almost entirely suppressed by the DTTF.

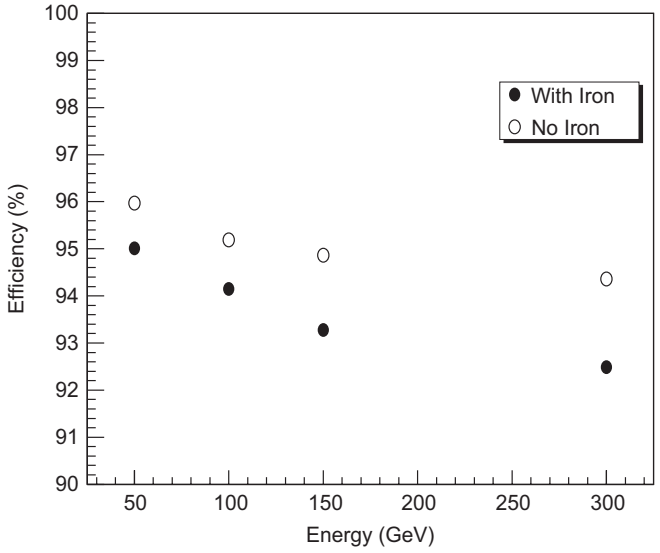

Fig. 8. BX identification efficiency in MB3 as a function of the incident muon momentum, for events with and without the iron absorber placed in front of MB3.

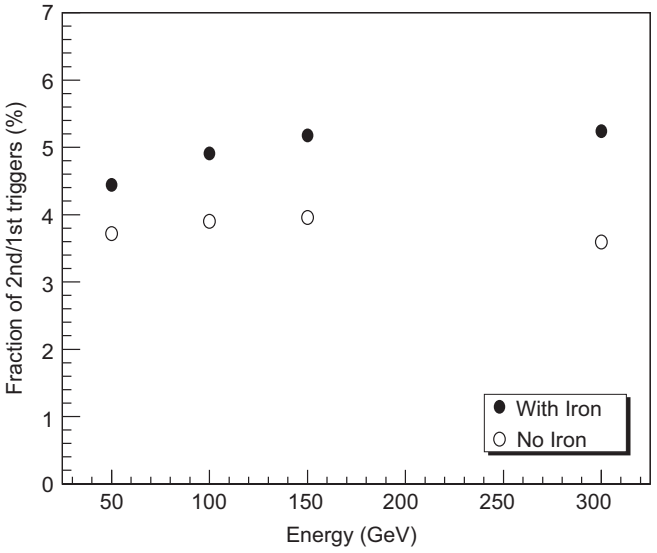

Fig. 9. Fraction of ghost triggers observed in MB3, defined as the ratio of the number of second tracks over the number of first tracks, delivered by the local trigger at the correct BX, as a function of the muon momentum, for events with and without the iron absorber.

a role. Finally, there were small occasional variations in the synchronization of the electronics during the data taking, that may induce a small variation of the trigger efficiency.

From the point of view of the PHTF algorithm, also trigger segments occurring at the BX adjacent to the correct one can be used to form a track trigger candidate, if a proper matching with segments at other muon stations is achieved. Therefore, such trigger segments occurring at the "wrong" BX can still contribute to the effective DTTF trigger efficiency (defined as the probability of the DTTF to reconstruct a trigger candidate), if they reproduce the correct inclination and position of the incident muon track. A dedicated analysis showed that, when the iron absorber is placed between the two stations, the effective efficiency of the down-stream station increases by only about 0.5% when also such "wrong BX" trigger segments are taken into account. This becomes only about 0.3% in the case of no absorber.

The fraction of ghost triggers at correct BX as a function of incident muon momentum, and the fraction of out-of-time triggers, as defined above, are shown, respectively, in Figs. 9 and 10 as a function of the incident muon momentum, for events with and without the iron absorber.

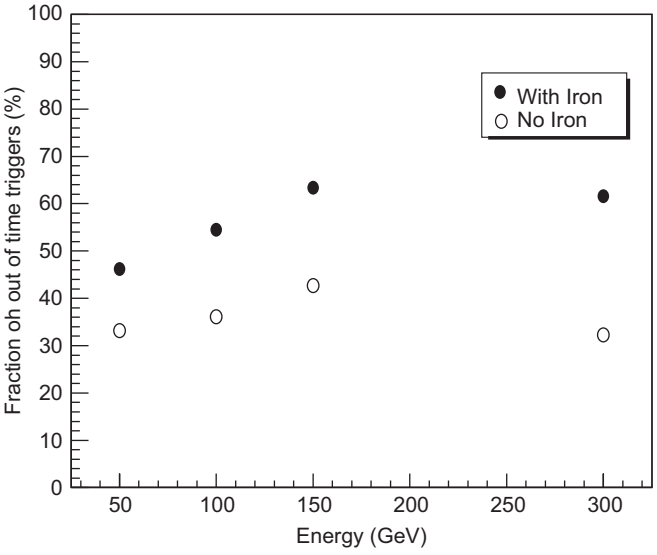

Fig. 10. The fraction of out-of-time triggers in MB3, defined as the number of out-of-time trigger segments divided by the number of selected single muon events, as a function of the muon momentum, for events with and without the iron absorber.

5.2. PHTF results

In the real CMS detector a muon track crossing the MB1 station with a given inclination and at a given point, has a well defined transverse momentum. With the present test beam set-up, muon tracks cross the MB1 station orthogonally, and their impact point is not fixed, but it depends on the beam spread, which is of the order of few centimeters. Taking as a guideline Fig. 2, for a given impact point of the incident track in MB1, expressed by the quantity ϕ, there is a precise relation between its bending angle ϕ_b in MB1, and the expected angle ϕ in MB3. This holds also for the present experimental set-up. If we call $\Delta\phi$ the difference between ϕ in MB1 and MB3, the tracks which cross the two muon stations are expected to fall within the narrow band of Fig. 11. Therefore, among all the possible DT trigger segments released by the two muon stations, only those which have bending angles which fall in such band can be successfully matched by the PHTF algorithm to form a trigger track. The beam spread in this case simulates a spread of transverse momentum values. In the same figure the points which correspond to the

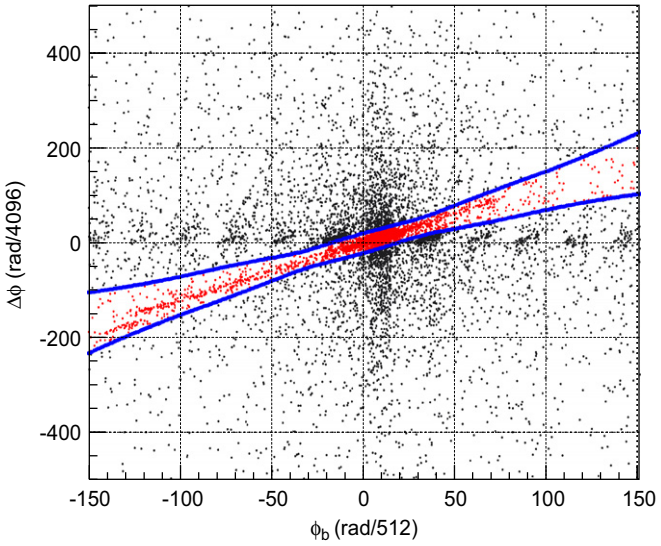

Fig. 11. Difference $\Delta\phi$ between the two values ϕ of the trigger segment in MB1 and MB3, as a function of the value ϕ_b in MB1. The reconstructed PHTF tracks lie in the narrow band where the extrapolation is allowed, as expected. The other points are wrong associations, and are not reconstructed by the PHTF algorithm.

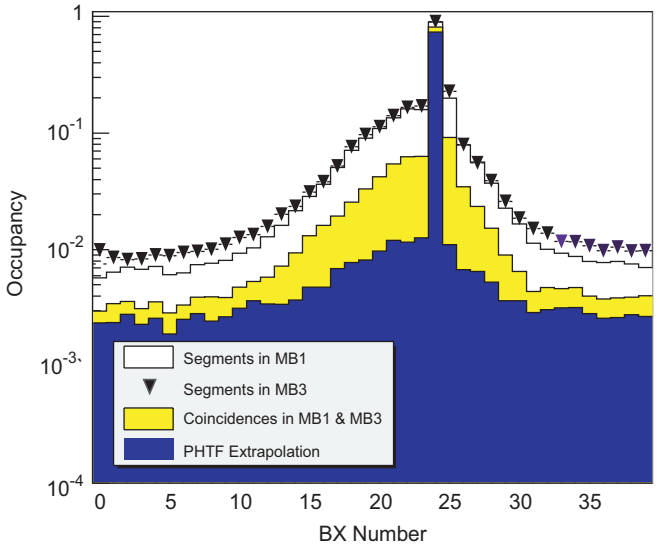

Fig. 12. Distribution of the BX assigned to the tracks found by the PHTF. The BX is correctly identified when its value is 24. Superimposed are the distributions of the same quantity determined independently by the local trigger in MB1 and MB3, as well as the distribution of the determined BX when a trigger segment at the same BX was delivered in coincidence in MB1 and MB3.

successful extrapolations, all lay within the expected range. Other points represent all the cases with two trigger segment, one in each station, which were not matched by the PHTF extrapolation. For the analysis of the DTTF results, first all the events which gave the trigger-scintillators coincidence were analyzed, without any further selection cut.

Fig. 12 shows the distribution of the BX assigned to the tracks found by the PHTF. The BX is correctly identified when its value is 24. Superimposed are the distributions of the same quantity determined independently by the local trigger in MB1 and MB3, as well as the distribution of the determined BX when a trigger segment with the same BX was delivered in coincidence in MB1 and MB3. It can be seen that the PHTF is fully efficient to deliver track candidates at the correct BX, whereas for out-of-time triggers the corresponding PHTF trigger rate is suppressed at the level of 1% or less.

A large fraction of the out-of-time triggers is due to real muons crossing the experimental apparatus at a BX different from 24, and which are correctly reconstructed by the PHTF. This is confirmed by the fact that the trigger segments which are matched together to form such tracks, are mainly of the type HH, thus indicating the passage of a real muon track. Fig. 13 shows the PHTF efficiency to reconstruct a trigger track in events with a MB1 and MB3 coincidence, as a function of the BX. Superimposed are the efficiency to reconstruct a trigger track when the two trigger segments are both of HH type, and both of L quality, respectively. The correct BX is 24. The PHTF efficiency for HH coincidences is $99.7 \pm 0.1\%$ and is practically constant for any BX. This fits with the expectations, as such tracks are real muons crossing the

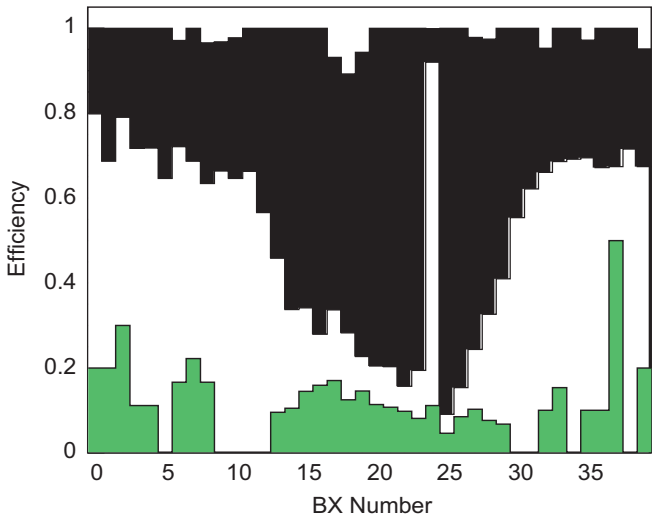

Fig. 13. Efficiency to reconstruct a trigger track by the PHTF, as a function of the BX (white), in events with a MB1–MB3 coincidence. The correct BX is 24. Superimposed are the efficiency to reconstruct a trigger track when there is a coincidence of two trigger segments both of HH quality (black), and a coincidence of two trigger segments both of L quality (light gray).

apparatus. On the other hand, when the trigger segments have a low quality, which is typical of fake triggers, the PHTF ghost suppression is very effective. The rejection power for ghosts (L coincidences at $BX \neq 24$) is 9.5 ± 0.4. Therefore, although the out-of-time local trigger rate in a single station is rather high (as shown in Figs. 7 and 10), the PHTF is very effective in the ghost rejection.

After validating the extrapolation principle, we measured the PHTF extrapolation efficiency as a function of

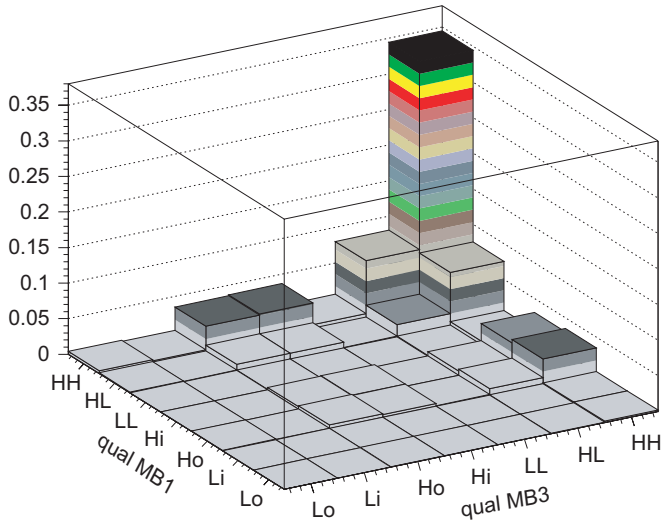

Fig. 14. Correlation between the quality of the local trigger segment in MB1 (qual MB1) versus MB3 (qual MB3), for events with a PHTF trigger track at the correct BX.

the input segment quality. We selected events with only one local trigger segment in both MB1 and MB3 in BX = 24, and with position within ±5 cm from the scintillator trigger. Fig. 14 is a lego plot which shows the correlation between the quality of the local trigger segment in MB1 versus MB3. The relative occupancies in the plot for correlated–correlated, correlated–non-correlated, non-correlated–correlated and non-correlated–non-correlated input segments, (where the first segment refers to MB1 and the second to MB3), are, respectively $(78.9 \pm 0.2)\%$, $(9.8 \pm 0.2)\%$, $(9.7 \pm 0.2)\%$ and $(1.6 \pm 0.1)\%$. The efficiency is defined as the fraction of such events with also a PHTF output trigger track. The extrapolation efficiencies corresponding to the relative occupancies listed above are $(99.9 \pm 0.1)\%$, $(99 \pm 1)\%$, $(84 \pm 1)\%$ and $(79 \pm 2)\%$, respectively. The overall PHTF extrapolation efficiency, averaged over all cases, is $(97.9 \pm 0.1)\%$, in agreement with the DTTF design requirements.

6. Conclusions

Two DTs muon stations of the CMS muon barrel system were exposed, in October 2004, to a 40 MHz bunched muon beam at the CERN SPS. The performance of the Level-1 local trigger was tested at different energies and inclination angles of the incident muon beam. Data with and without an iron absorber placed between the two stations were also collected, to simulate the electromagnetic shower development in CMS. The effect of the absorber is to decrease the BX identification efficiency by about 3%, when the muon momentum is increased from 50 to 300 GeV, due to the development of electromagnetic showers. Special data-taking runs were dedicated to test for the first time the PHTF trigger. The analysis results showed in all cases excellent agreement to the design performance requirements, in particular high efficiency to reconstruct tracks at the correct BX, as well as good rejection power to discard ghosts.

Acknowledgments

We acknowledge the support of the staff of the Electronics and Mechanical Workshop of INFN Bologna, INFN Padova, RWTH Aachen and CIEMAT. In particular we are grateful to L. Barcellan and G. Fetchenhauer for their valuable technical help. We acknowledge the help G. Bencze who provided the scintillator setup used as external muon trigger. We also acknowledge the financial support of the Spanish Ministerio de Educación y Ciencia. Furthermore we acknowledge the support by the German "Bundesministerium für Bildung und Forschung" (BMBF).

References

[1] CMS, Technical Proposal, CERN/LHCC 94-38, LHCC/P1, 1994.
[2] CMS, The Muon Project, Technical Design Report, CERN/LHCC 97-32.
[3] CMS, The Level-1 Trigger, Technical Design Report, CERN/LHCC 2000-038.
[4] P. Arce, et al., Nucl. Instr. and Meth. A 534 (2004) 441.
[5] M. Aguilar-Benitez, et al., Nucl. Instr. and Meth. A 480 (2002) 658 and references therein.
[6] B. Taylor, IEEE Trans. Nucl. Sci. NS-45 (1998).
[7] G.M. Dallavalle, et al., Proceedings of the Fourth Workshop on Electronics for LHC Experiments, Rome, September 1998.